View metadata, citation and similar papers at core.ac.uk
brought to you by CORE
provided by CiteSeerX

Structural and Optical Properties of $Ge_{1-x}Sn_x$ Alloys Grown on GaAs (001) by R. F. Magnetron Sputtering

H. Pérez Ladrón de Guevara [a], A. G. Rodríguez[b], H. Navarro-Contreras[b], and M. A. Vidal[b]

[a] Centro Universitario de los Lagos, Universidad de Guadalajara, Av. Enrique Díaz de León 1144, col. Paseos de la Montaña, Lagos de Moreno, Jalisco 47460, México
[b] Coordinación para la Innovación y la Aplicación de la Ciencia y la Tecnología (CIACYT), Universidad Autónoma de San Luís Potosí (UASLP), Álvaro Obregón 64, San Luis Potosí, S L P 78000, México

$Ge_{1-x}Sn_x$ alloys were grown on GaAs (001) substrates in a conventional R. F. magnetron sputtering system with two independent plasmas not simultaneous focus to substrate. We determined the in-plane and in-growth lattice parameters for different Sn concentrations by high resolution X-ray diffraction (HRXRD). We observed that $Ge_{1-x}Sn_x$ layers with low Sn concentrations have pseudomorphic characteristics. But this layers relax at Sn concentrations higher than the ones growth on Ge (001) substrates. Raman spectroscopy confirms the Sn concentrations of the $Ge_{1-x}Sn_x$ layers.
We also determined the band gap transitions and we found that the indirect-direct band gap crossover occurs as is predicted in $Ge_{1-x}Sn_x$ alloys growth on Ge (001).

In modern semiconductor physics $Ge_{1-x}Sn_x$ alloys represents the realization of a direct energy-gap material based fully on group IV elements. Single crystal $Ge_{1-x}Sn_x$ alloys have interesting optical and electrical properties. It is experimentally reported that their fundamental band gap transforms from indirect to direct for x larger than 0.10 (1-6) even it is theoretically predicted than this transition occurs at lower Sn concentrations (7,8). These alloys are expected for developing optoelectronic infrared materials systems. In addition, $Ge_{1-x}Sn_x$ would be expected to exhibit high carrier mobility because of a lower effective mass than that of Ge and the lack of polar optical scattering (1,9) inherent to III–V materials. However there are several challenges associated with the synthesis of these alloys due to the limited bulk solubility exhibited by Sn in Ge ($x < 0.005$), a large lattice mismatch between Sn and Ge of 14.7% and lower surface free energy of Sn versus Ge leading to the surface segregation of Sn. To overcome Sn surface segregation it is necessary to grow at low temperatures, typically around 200 °C where it is possible to obtain single crystal $Ge_{1-x}Sn_x$ epitaxial thin films (2,3,10). Additionally, the maximum equilibrium solid solution of α-Sn in Ge and Ge in α-Sn is less than 1 and 0.6%, respectively (11). However the growth of these alloys in nonequilibrium conditions allowed us to obtain single phase $Ge_{1-x}Sn_x$ alloys with Sn concentrations between x = 0.01 to 0.14 on Ge (001) substrates by using a R. F. Magnetron Sputtering (12).

$Ge_{1-x}Sn_x$ layers has been used as buffer layers in order to integrate group IV an III-V elements such as Si (13-16) and GaAs (17). At the moment no one is trying to use III-V

Downloaded on 2016-10-05 to IP 130.203.136.75 address. Redistribution subject to ECS terms of use (see ecsdl.org/site/terms_use) unless CC License in place (see abstract).

substrates in this integration even exists some tryouts (18). In this work we report the growth of $Ge_{1-x}Sn_x$ alloys on GaAs (001) substrates. We start from the consideration that exists a lattice mismatch very close to the $Ge_{1-x}Sn_x$ /Ge (001) system. GaAs has a lattice constant of 5.6535 Å and present a lattice mismatch of 14.78% with the α-Sn. So growth conditions could be similar to the ones used in Ge (001) substrates as previously reported (12).

$Ge_{1-x}Sn_x$ metastable alloys were epitaxially grown on Ge(001) and GaAs(001) substrates in a R.F. planar magnetron sputtering system with a base pressure better than 10-7 mbar. Two independent Ar ~99.999% glow discharges were maintained to pulverize two water cooled Ge ~99.999% and Sn ~99.999% targets. Prior to the growth Ge substrates were cleaned using a degassing process (trichloroethylene, acetone, methanol, deionized water and Nitrogen dried) and an UV exposure for 30 min (19). GaAs substrates only were degassed and dried. In order of growing the $Ge_{1-x}Sn_x$ alloys in the same conditions. Both types of substrates were simultaneously attached in a molybdenum substrate holder. The substrates were introduced into the growth chamber from a load chamber and were heated to remove surface oxides. After a 30 min annealing, the substrates were cooled to the growth temperature (150 °C - 250 °C). During the cooling processes a Ge buffer layer was grown. The alloys were grown by varying the targets power, and the exposure time under the different plasmas. These conditions allowed us to change the Sn concentration in the alloys.

High Resolution X Ray Diffraction (HRXRD) in the symmetric reflection (004) was measured in all samples by using a Philips X'Pert MRD high-resolution X-ray diffractometer with a four-bounce Bartels Ge (2 2 0) monochromator. In order to determine the bulk lattice parameter it was necessary to obtain the in-plane and in-growth lattice parameters ($a^{\perp}$ and $a\|$). We used the asymmetric reflections (115) and (-1-15). The Sn concentration was obtained from the bulk lattice parameter.

Figure 1 shows typical rocking curves of $Ge_{1-x}Sn_x$ layers growth on GaAs (001) substrates around the (004) reflection at different Sn concentrations. The separation between the diffraction peaks of the substrate and the $Ge_{1-x}Sn_x$ layers increases conforming the Sn concentration also increases. We obtained Sn concentrations as low as 0.01 and also we obtained several alloys with a range of Sn concentration between 0.06 and 0.10 as is shown in the figure 1. We observed that the Sn concentration slightly varied in the alloys growth on different substrates. The maximum Sn concentration obtained by using GaAs (001) substrates was less than 0.10 instead of 0.14 on Ge (001) substrates.

Figure 2 shows the behavior of the in-plane and in-growth lattice parameters of the $Ge_{1-x}Sn_x$ alloys growth on GaAs (001) substrates compared with the results obtained for the $Ge_{1-x}Sn_x$ alloys growth on Ge (001) substrates (12). We already found the same relaxation process previously observed on Ge (001) substrates, but we obtain fully relaxed films at different Sn concentrations on each substrate. We observe that in the case of the alloys growth on GaAs (001) substrates, the $Ge_{0.99}Sn_{0.01}$ layer is fully strained as the alloys with a Sn concentration less than 0.04 growth on Ge (001) substrates. But conforming the Sn concentration increases the relaxation process occurs. The bulk lattice parameter increases and The in-plane and in-growth lattice parameters begin to close to increased bulk lattice parameter.

We assume that the small difference between the lattice mismatch of the GaAs (001) substrate on the Ge buffer layer and the $Ge_{1-x}Sn_x$ alloy induces a residual strain that can be responsible for the change in the relaxation process of the $Ge_{1-x}Sn_x$ films and in the

Downloaded on 2016-10-05 to IP 130.203.136.75 address. Redistribution subject to ECS terms of use (see ecsdl.org/site/terms_use) unless CC License in place (see abstract).

final Sn concentration of the alloy. Also a strain due to differences in the linear thermal expansion coefficient (LTEC) between the system $Ge_{1-x}Sn_x$, Ge buffer layer and Ge (001) or GaAs (001) substrates could be considered.

Figure 3 shows the Raman spectra of the $Ge_{1-x}Sn_x$ alloys growth on GaAs (001) substrates. This figure indicates in dashed lines the position of the LO and TO modes of Ge and GaAs. The peak position is clearly shifted from the Ge position. The Raman shift increases as the Sn concentration (determined by HRXRD) also increases.

In order to determinate the optical transitions of the $Ge_{1-x}Sn_x$ alloys, we use a FFT-IR spectrometer in a vacuum environment at room temperature. The film transmittance was obtained by dividing the measured transmittance signal by the substrate and Ge buffer layer transmittance signal. The absorption coefficient was obtained from the transmittance measurements.

Figure 4 shows the direct and indirect energy gap values obtained for the $Ge_{1-x}Sn_x$ allows grown on GaAs (001) substrates compared with the previously reported behavior of the direct and indirect energy gaps (3, 4). We also observed that the transition between indirect to direct energy gap semiconductor occurs around a critical Sn concentration of 0.09.

In conclusion we have shown that it is possible to grow single phase $Ge_{1-x}Sn_x$ layers on GaAs (001) substrates by using a R.F. Magnetron Sputtering system. This layers relax at Sn concentrations higher that the ones grown on Ge (001) substrates. The indirect to direct energy band gap transition occurs around the experimental Sn critical concentration previously reported.

Downloaded on 2016-10-05 to IP 130.203.136.75 address. Redistribution subject to ECS terms of use (see ecsdl.org/site/terms_use) unless CC License in place (see abstract).

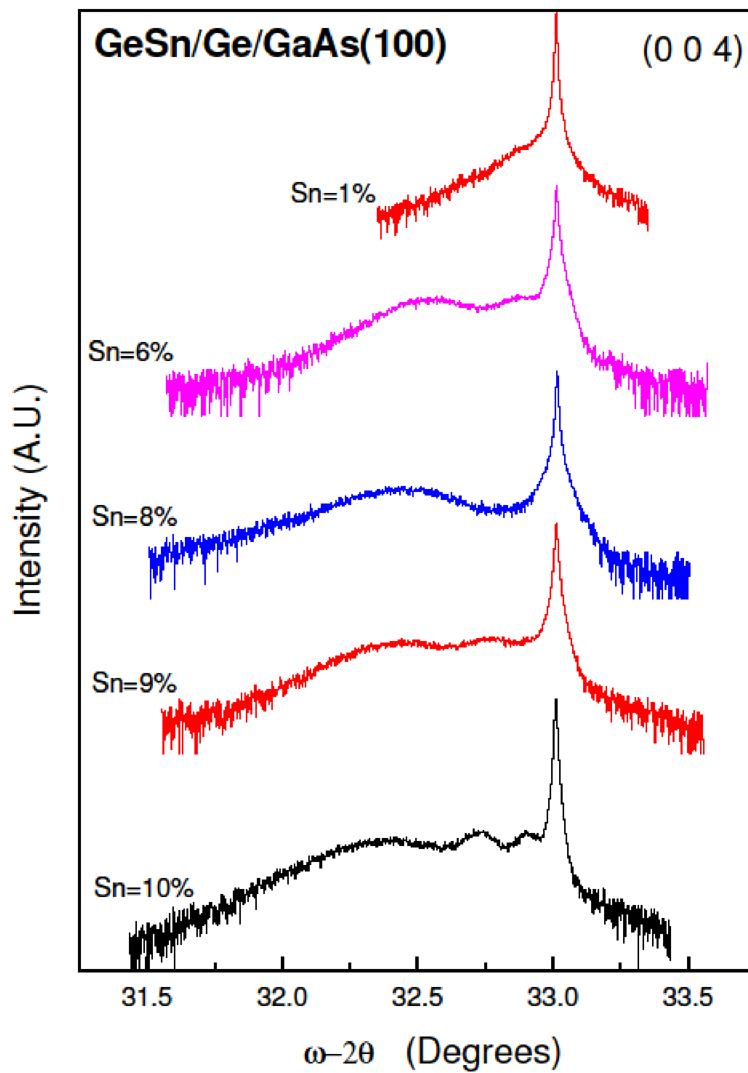

Figure 1. (004) Rocking curves of $Ge_{1-x}Sn_x$ layers growth on GaAs (001) substrates at different Sn concentrations.

Downloaded on 2016-10-05 to IP 130.203.136.75 address. Redistribution subject to ECS terms of use (see ecsdl.org/site/terms_use) unless CC License in place (see abstract).

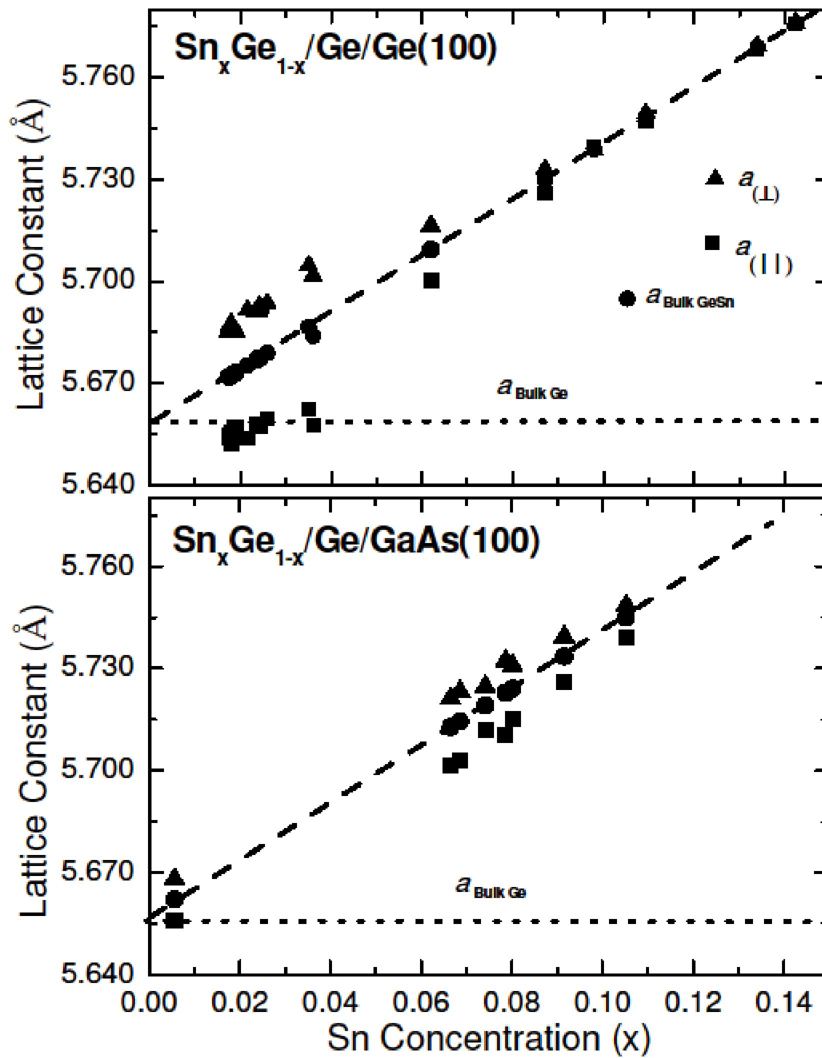

Figure 2. Behavior of the in-plane and in-growth lattice parameters of the $Ge_{1-x}Sn_x$ layers growth on GaAs (001) and Ge (001) substrates (12). We observe that the relaxation process occurs at different Sn concentrations.

Downloaded on 2016-10-05 to IP 130.203.136.75 address. Redistribution subject to ECS terms of use (see ecsdl.org/site/terms_use) unless CC License in place (see abstract).

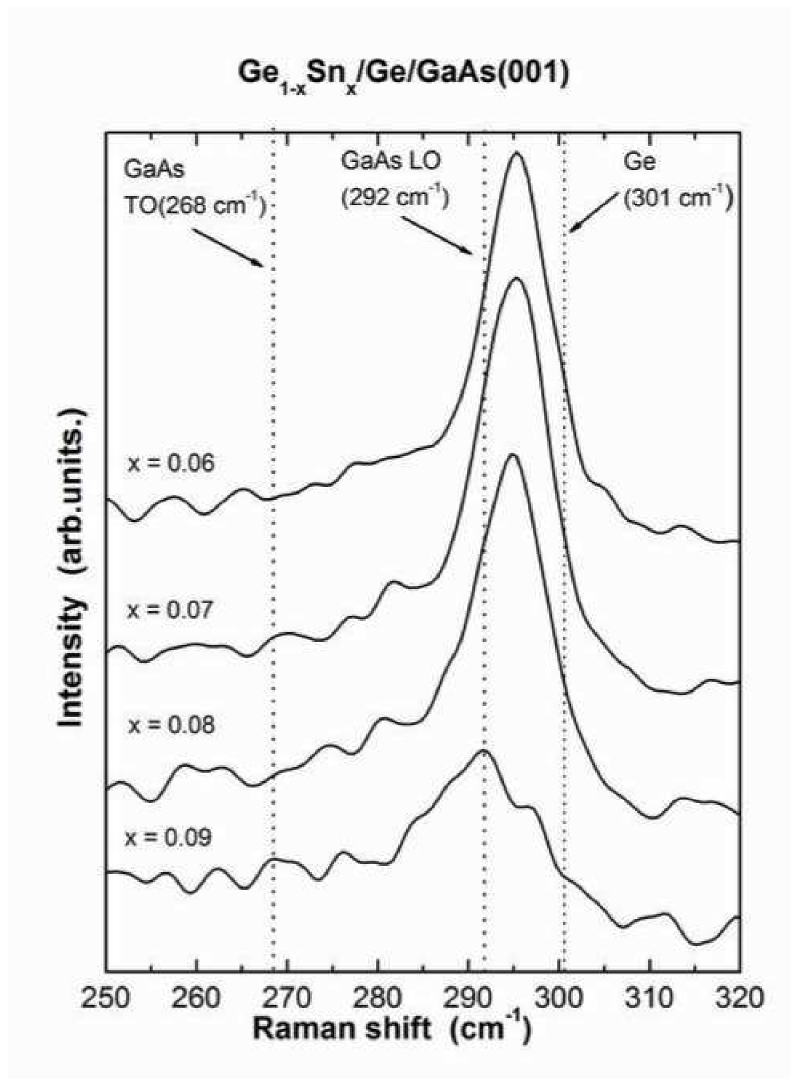

Figure 3. Raman spectra of R. F. Magnetron Sputtered grown thin films of $Ge_{1-x}Sn_x$/Ge(100)/GaAs. The Sn concentration is established by HRXRD.

Downloaded on 2016-10-05 to IP 130.203.136.75 address. Redistribution subject to ECS terms of use (see ecsdl.org/site/terms_use) unless CC License in place (see abstract).

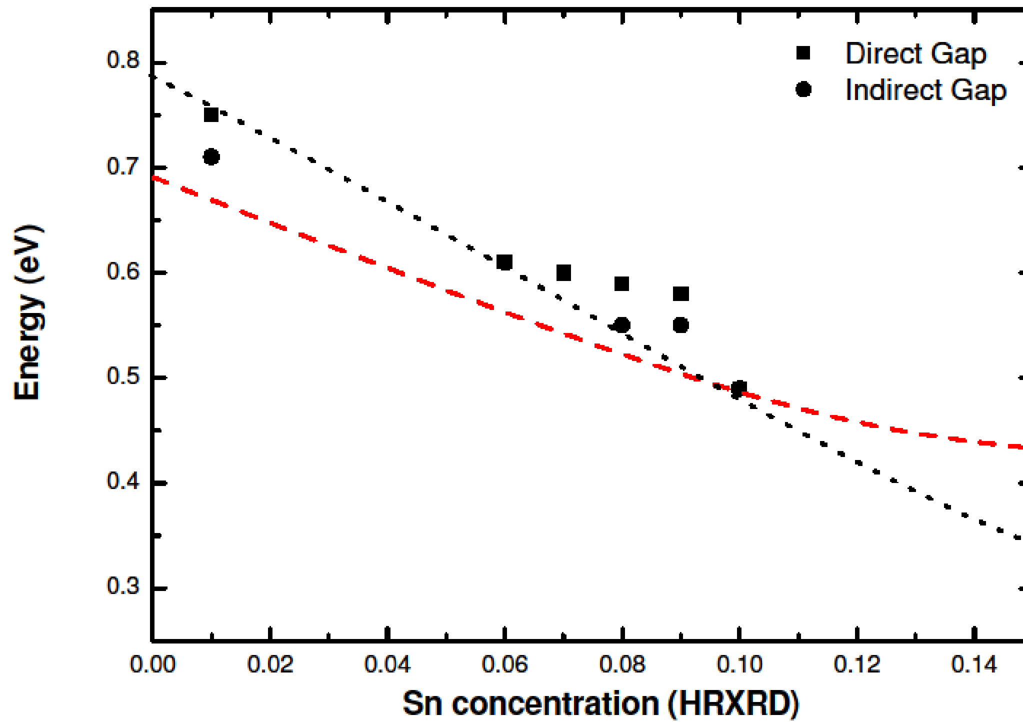

Figure 4. Experimental direct and indirect energy gap values obtained for the $Ge_{1-x}Sn_x$ allows grown on GaAs (001) substrates compared with the theoretical and experimental behavior curves previously reported (3, 4).

Downloaded on 2016-10-05 to IP 130.203.136.75 address. Redistribution subject to ECS terms of use (see ecsdl.org/site/terms_use) unless CC License in place (see abstract).

Acknowledgments

The authors hereby wish to acknowledge the financial support from Consejo Nacional de Ciencia y Tecnología (CONACyT) México, during the course of this research.

References

1. D. W. Jenkins and J. D. Dow, *Phys. Rev. B*, **36**, 7994 (1987).
2. G. He and H. A. Atwater, *Phys. Rev. Lett.*, **79**, 1937 (1997).
3. R. Ragan and H. A. Atwater, *Appl. Phys. Lett.*, **77**, 3418 (2000).
4. H. P. L. de Guevara, A. G. Rodriguez, H. Navarro-Contreras, and M. A. Vidal, *Appl. Phys. Lett*,. **84**, 4532 (2004).
5. V. R. D'Costa, C. S. Cook, A. G. Birdwell, C. L. Littler, M. Canonico, S. Zollner, J. Kouvetakis, and J. Menendez, *Phys. Rev. B*, **73**, 125207 (2006).
6. M. Coppinger, J. Hart, N. Bhargava, S. Kim and J. Kolodzey, *Appl. Phys. Lett.*, **102**, 141101 (2013).
7. A. A. Tonkikh, C. Eisenschmidt, V. G. Talalaev, N. D. Zakharov, J. Schilling, G. Schmidt and P. Werner, *Appl. Phys. Lett.*, **103**, 032106 (2013).
8. V. R. D'Costa, C. S. Cook, A. G. Birdwell, C. L. Littler, M. Canonico, S. Zollner, J. Kouvetakis, and J. Menéndez, *Phys. Rev. B*, **73**, 125207 (2006).
9. S. I. Shah, J. E. Green, L. L. Abels, Q. Yao, and P. M. Raccah, *J. Cryst. Growth*, **83**, 3 (1987).
10. G. He and H. A. Atwater, *Appl. Phys. Lett.*, **68**, 664 (1996).
11. Bull. Alloy Phase Diagrams, and references therein, **5**, 266 (1984).
12. H. P. L. de Guevara, A. G. Rodriguez, H. Navarro-Contreras, and M. A. Vidal, *Appl. Phys. Lett.*, **83**, 4942 (2003).
13. M. Bauer, J. Taraci, J. Tolle, A. V .G. Chizmeshya, S. Zollner, David J. Smith, J. Menéndez, Changwu Hu, and J. Kouvetakis, *Appl. Phys. Lett.*, **81**, 2992 (2002).
14. V. R. D'Costa, Y.-Y. Fang, J. Tolle, J. Kouvetakis, and J. Menendez, *Phys. Rev. Lett.*, **102**, 107403 (2009).
15. G. Sun, R. A. Soref, and H. H. Cheng, *J. Appl. Phys.*, **108**, 033107 (2010).
16. S. Su, B. Cheng, C. Xue, W. Wang, Q. Cao, H. Xue, W. Hu, G. Zhang, Y. Zuo, Q. Wang, *Optics Express*, **19**, 6400 (2011).
17. R. Roucka, J. Tolle, C. Cook, A. V. G. Chizmeshya, J. Kouvetakis, V. D'Costa, J. Menendez, Zhihao D. Chen and S. Zollner, *Appl. Phys. Lett.*, **86** , 191912 (2005).
18. S. I. Shah, J. E. Greene, L. L. Abels, Q.Yao and P. M. Raccah, *J. Crystal Growth*, **83**, 3 (1987).
19. X. J. Zhang, G. Xue, A. Agarwal, R. Tsu, M. A. Hassan, J. E. Greene, and A. Rockett, *J. Vac. Sci. Technol. A*, **11**, 2553 (1993).

Downloaded on 2016-10-05 to IP 130.203.136.75 address. Redistribution subject to ECS terms of use (see ecsdl.org/site/terms_use) unless CC License in place (see abstract).